

Acoustic Excitation on the Flow Over a Low-Re Airfoil," *Journal of Fluid Mechanics*, Vol. 182, Sept. 1987, pp. 127-148.

³Hsiao, F. B., Liu, C. F., and Shyu, J. Y., "Control of Wall-Separated Flow by Internal Acoustic Excitation," *AIAA Journal*, Vol. 28, No. 8, 1990, pp. 1440-1446.

⁴Chang, R. C., Hsiao, F. B., and Shyu, R. N., "Forcing Level Effect of Internal Acoustic Excitation on the Improvement of Airfoil Performance," *Journal of Aircraft*, Vol. 29, No. 5, 1992, pp. 823-829.

⁵Roshko, A., "On Drag and Shedding Frequency of Two-Dimensional Bluff Bodies," NACA-TN-3169, 1954.

⁶Blevins, R. D., "The Effect of Sound on Vortex Shedding From Cylinders," *Journal of Fluid Mechanics*, Vol. 161, Dec. 1985, pp. 217-237.

Using the Liou-Steffen Algorithm for the Euler and Navier-Stokes Equations

Lorenzo Bergamini* and Pasquale Cinnella†

Mississippi State University,
Mississippi State, Mississippi 39762

Introduction

RECENT years have witnessed the affirmation of both flux-vector and flux-difference techniques¹ for the accurate numerical simulation of compressible fluid flows. Two of the most popular schemes have been proposed by Roe and Van Leer, respectively, and are widely utilized for both inviscid and viscous calculations. However, robustness problems have been experienced by some users of the Roe scheme,² and the Van Leer technique has been shown to be too dissipative for viscous calculations.³

In a related study,⁴ the authors investigated the advantages and drawbacks of a new flux-splitting scheme proposed by Liou and Steffen,³ when compared with the algorithms developed by Van Leer and Roe. The comparison involved inviscid and viscous flows in one and two space dimensions. In the following, a brief summary of those findings is given.

Numerical Formulation

The governing equations for viscous flows are discretized in space using upwind technology, in conjunction with a finite volume approach.⁵ Three different flux-splitting schemes are implemented for the discretization of the inviscid fluxes, and second-order central differences are utilized for the viscous fluxes.

Two different techniques have been implemented to advance the numerical solution in time: an explicit m -step Runge-Kutta algorithm⁵ and a fully implicit modified two-step factorization technique.⁶ The Runge-Kutta algorithm with two or more steps is second-order accurate in time and is particularly useful for unsteady simulations. The implicit formulation can be made second-order accurate in time by means of inner iterations to the unsteady residual.⁶

The convergence rate to steady-state solutions is enhanced by means of mesh sequencing, whereby the computation is started impulsively on a coarse grid, and after a convenient residual reduction, the partially converged solution is extrapolated to a finer grid. This technique allows for an inexpensive resolution of the initial transient, which is typically responsible for a large portion of the total CPU time required for a given simulation.

Three flux-splitting schemes are compared in the following. The first one was originally proposed¹ by Van Leer. The second one was proposed by Liou and Steffen,³ is similar to Van Leer's, and is also based on the splitting of a velocity parameter and the pressure.

Presented as Paper 93-0876 at the AIAA 31st Aerospace Sciences Meeting, Reno, NV, Jan. 11-14, 1993; received March 13, 1993; revision received Aug. 10, 1993; accepted for publication Aug. 25, 1993. Copyright © 1993 by the American Institute of Aeronautics and Astronautics, Inc. All rights reserved.

*Research Assistant, Engineering Research Center for Computational Field Simulation, P.O. Box 6176.

†Assistant Professor, Department of Aerospace Engineering, P.O. Box 6176. Member AIAA.

The splitting formulas are the same ones employed by the previous scheme, although a lower-order splitting for the pressure is introduced and recommended by the authors over the "standard" formula. The algorithm differs from the previous one in the treatment of the convective contributions to the inviscid fluxes. Finally, an approximate Riemann solver of the Roe type¹ is implemented and compared with the previous techniques.

Numerical Results

Numerical results for seven test cases, four inviscid and three viscous, were obtained in a related study.⁴ The explicit two-step Runge-Kutta time integration scheme was adopted for the unsteady cases and the fully implicit modified two-step algorithm for the steady results. Unless otherwise stated, the space discretization was second-order accurate. The Van Leer limiter⁶ was employed to correct the extrapolation of the primitive variables, which is necessary for the determination of left and right states to be utilized in the splitting algorithms, according to a Monotone Upstream-Centered Schemes for Conservation Laws (MUSCL) type logic.⁷

In the following, the major features of two of those test cases will be detailed.

Shock Reflection off of a Solid Wall

A shock tube simulation was selected as a simple unsteady test case with a known exact solution. The pressure and density ratios were selected to be 10:1, consequently, the temperature ratio between driver and driven sections was 1. The calculation utilized 400 points over a distance of 1 m, with the initial discontinuity located at a distance of $x=0.25$. The nondimensional time step utilized to advance the solution was $\Delta t=5 \times 10^{-4}$, and the reference values chosen for the nondimensionalization were the density and speed of sound in the driven section. The maximum Courant-Friedrichs-Lewy (CFL) number registered was of the order of 0.4.

The calculation was continued until the shock reached the end of the tube and reflected off of it. A solid wall boundary condition was imposed. Both characteristic-variable boundary conditions⁸ and a straightforward imposition of zero pressure gradients/zero velocity at the wall were implemented, and the final results were insensitive to the choice made. The same boundary conditions were employed for all three techniques.

Figure 1 shows temperature plots for the three schemes at a nondimensional time $t=0.6$, which corresponds to conditions after reflection at the wall but before impact between the reflected shock and the contact discontinuity; Fig. 2 depicts temperature at time $t=0.725$, after the impact with the contact discontinuity but before contact with the expansion region. The light line represents the exact solution. The heavy line represents the prediction from

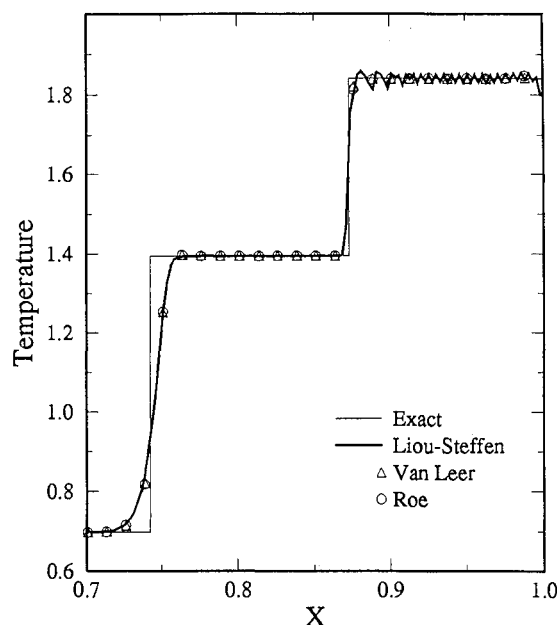


Fig. 1 Temperature distribution in the shock tube at $t=0.6$.

the Liou-Steffen algorithm, and the symbols correspond to Roe's and Van Leer's schemes (only one point in five is shown). The results show two distinct periodic oscillations. The first one, with a period of 12–15 cells, is present in all three schemes in the wake of the reflected shock and is damped in 4 to 5 periods. The second one has a period of two cells, is superimposed on the first one, and appears only in the Liou-Steffen scheme. This latter oscillation is not attenuated.

To eliminate the possibility that the boundary condition at the wall could have affected the results, we performed a simulation with the solid wall replaced by an additional shock tube symmetric to the first one. This resulted in two equal and opposite shocks colliding at the location of the original solid wall. The results for this run were identical to those obtained with the solid wall. Calculations performed with the MINMOD limiter have resulted in the same overall behavior. Changing the pressure splitting from the low-order polynomial to the higher-order formula³ yielded further deterioration of the Liou-Steffen results. Finally, a run performed using a Newton relaxation implicit algorithm with second-order time accuracy⁶ resulted in a solution essentially equivalent to the explicit one.

The possibility that the MUSCL extrapolation technique might be responsible for the high-frequency oscillations is currently being investigated.

Laminar Flat Plate

The laminar flat plate is a useful preliminary test of the ability of the different discretizations to yield accurate solutions in the presence of viscous phenomena. The predictions obtained from the three algorithms were compared with the Blasius solution. Although the latter is valid for incompressible flows, it is a reasonable approximation of compressible flows with subsonic freestream Mach numbers. The conditions selected for the test case are Mach number $M_\infty = 0.5$, Reynolds number based on the flat plate length $Re = 1 \times 10^4$, and Prandtl number $Pr = 0.72$. The computational domain extends five plate lengths upstream, downstream, and orthogonally to the plate. A mesh of 81 points in the freestream direction, 50 of which are located on the plate, and 41 points in the orthogonal direction is used. The stretching of the grid in the normal direction was varied to obtain a fine mesh, with a cell Reynolds number of 1×10^1 and 12–15 points in the boundary layer, and a coarse mesh, with a cell Reynolds number of 1×10^2 and only 3–4 points in the boundary layer. The results for the fine mesh are in good agreement with the Blasius solution. The wall temperature obtained by means of the approximate formula

$$\frac{T_w}{T_\infty} = 1 + \sqrt{Pr} \frac{(\gamma - 1)}{2} M_\infty^2 \quad (1)$$

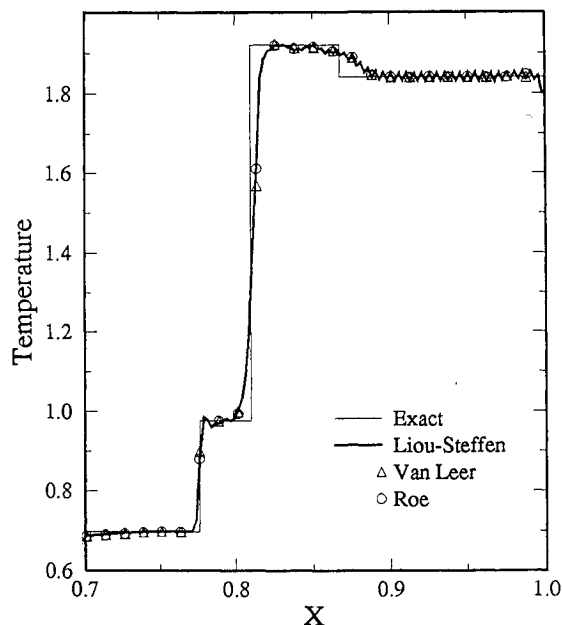


Fig. 2 Temperature distribution in the shock tube at $t = 0.725$.

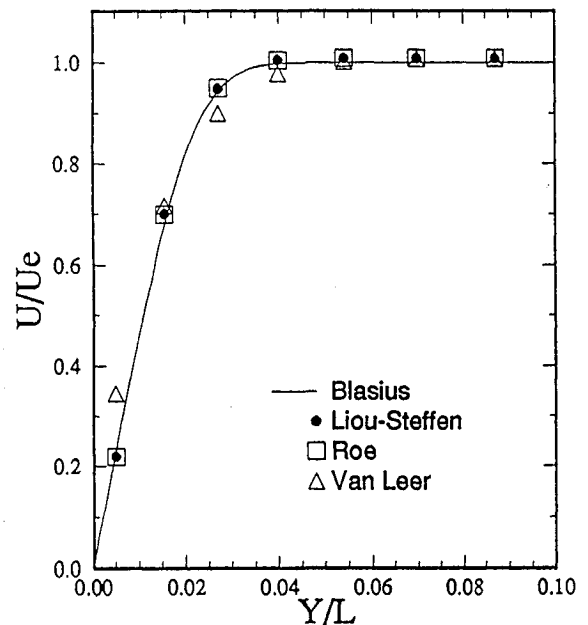


Fig. 3a Velocity profile over a laminar flat plate; coarse mesh.

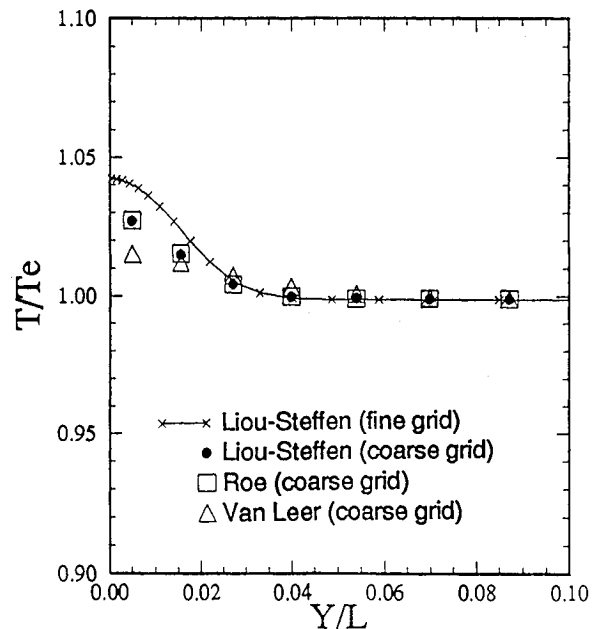


Fig. 3b Temperature profile over a laminar flat plate; coarse mesh.

results in the value $T_w/T_\infty = 1.042$, which is in excellent agreement with the computational solution.

The coarse grid solution, shown in Figs. 3a and 3b, features a satisfactory velocity profile for the Roe and Liou-Steffen algorithms and a less than ideal behavior by the Van Leer scheme, which has been found to be too dissipative for viscous solutions.³ The coarse grid predictions of the temperature show some degradation in accuracy, and again the Van Leer results are the worst. There is no significant difference between the Roe and Liou-Steffen algorithms.

Concluding Remarks

If the present investigation was a contest for the title of "best algorithm for the compressible Euler and Navier-Stokes equations," there would probably be no clear winner. On the negative side, the Roe scheme is not robust enough, especially for high-speed problems, the Van Leer technique is not accurate enough for viscous problems, and the Liou-Steffen algorithm shows a ten-

dency toward spurious oscillations in both viscous and inviscid problems. On the positive side, however, the Roe scheme is very accurate, the Liou-Steffen technique rivals that accuracy at a reduced cost, and the Van Leer algorithm can provide essentially nonoscillatory solutions for hypersonic flow conditions. The search for the optimal algorithm for compressible flows is probably still open.

Acknowledgments

This work was funded in part by the National Science Foundation, which supports the Engineering Research Center for Computational Field Simulation. The first author would like to acknowledge the partial support he obtained from the Polytechnic of Bari, Italy, while he was working at the Engineering Research Center.

References

- ¹Roe, P. L., "Characteristic-Based Schemes for the Euler Equations," *Annual Review of Fluid Mechanics*, Vol. 18, 1986, pp. 337-365.
- ²Peery, K. M., and Imlay, S. T., "Blunt-Body Flow Simulations," AIAA Paper 88-2904, July 1988.
- ³Liou, M.-S., and Steffen, C. J., Jr., "A New Flux Splitting Scheme," NASA TM 104404, May 1991.
- ⁴Bergamini, L., and Cinnella, P., "A Comparison of 'New' and 'Old' Flux-Splitting Schemes for the Euler Equations," AIAA Paper 93-0876, Jan. 1993.
- ⁵Cinnella, P., and Grossman, B., "Flux-Split Algorithms for Hypersonic Flows," *Computational Methods in Hypersonic Aerodynamics*, edited by T. K. S. Murthy, Computational Mechanics Publications, Southampton, England, UK, 1991, Chap. 5, pp. 150-202.
- ⁶Whitfield, D. L., Janus, J. M., and Simpson, L. B., "Implicit Finite Volume High Resolution Wave-Split Scheme for Solving the Unsteady Three-Dimensional Euler and Navier-Stokes Equations on Stationary or Dynamic Grids," Mississippi State Univ., EIRS Report MSSU-EIRS-ASE-88-2, Mississippi State, MS, Feb. 1988.
- ⁷Hirsch, C., *Numerical Computation of Internal and External Flows*, Vol. 2, Wiley, Chichester, England, UK, 1990.
- ⁸Whitfield, D. L., and Janus, J. M., "Three-Dimensional Unsteady Euler Equations Solution Using Flux Vector Splitting," AIAA Paper 84-1552, June 1984.

Differencing of Density in Compressible Flow for a Pressure-Based Approach

G. P. Greyvenstein* and J. P. Meyer†
Potchefstroom University for CHE,
Potchefstroom 2520, South Africa

Nomenclature

a	= coefficient in the discretization equation
p	= pressure
s	= source term
u	= x -direction velocity
x	= coordinate
y	= coordinate
z	= nozzle length
α	= weighing factor
Δt	= time step
Δx	= x -direction width of the control volume
ρ	= density

Subscripts

E	= neighbor in the positive x direction, i.e., on the eastern side
-----	---

e	= control-volume face between P and E
P	= central grid point under consideration
W	= neighbor in the negative y direction, i.e., on the western side
w	= control-volume face between P and W
$*$	= based on the guessed pressure
$'$	= corrected value

Superscripts

o	= old value
T	= for energy equations
U	= for momentum equation

Introduction

BECAUSE of the difference in nature between compressible and incompressible flows, different computational schemes have been developed through the years to deal with these two types of flows. In the case of compressible flows, methods have been developed that use density as a primary variable. Such methods are known as density-based methods. Examples of density-based methods are the well-known methods of MacCormack¹ and Beam and Warming.² Unlike density-based methods, pressure-based methods use pressure as a primary variable. Examples of pressure-based methods are the well-known SIMPLE³ and PISO⁴ methods.

The purpose of this paper is to investigate the differencing scheme of density used for the convection terms in the momentum transport equations. To provide a clear understanding, we will discuss these concepts in the framework of a one-dimensional scheme. Fortunately, all of these concepts as developed within this one-dimensional framework are readily extended to two or three dimensions.

Discretized Equations

Different methods can be used to discretize the equations of motion. In this paper the control-volume-based discretization scheme described by Patankar⁵ is applied. Discretization of continuity, momentum, and energy equations leads to the following algebraic equations:

$$y_P \Delta x \left(\frac{\rho_P - \rho_P^o}{\Delta t} \right) = (\rho_w u_w y_w - \rho_e u_e y_e) \quad (1)$$

$$a_P^u u_P = a_E^u u_E + a_W^u u_W - b_P^u (p_E - p_P) + s_P^u \quad (2)$$

$$a_P^T T_P = a_E^T T_E + a_W^T T_W + s_P^T \quad (3)$$

The solution of Eq. (2) using the guessed pressure field results in the following equation for tentative velocities:

$$a_P^u u_P^* = a_E^u u_E^* + a_W^u u_W^* - b_P^u (p_E^* - p_P^*) + s_P^u \quad (4)$$

If Eq. (4) is subtracted from Eq. (2), the following equation is obtained:

$$a_P^u u_P' = a_E^u u_E' + a_W^u u_W' - b_P^u (p_E' - p_P') \quad (5)$$

where u' is the velocity correction and p' is the pressure correction. The actual velocities and pressures are given by

$$u = u^* + u' \quad (6)$$

and

$$p = p^* + p' \quad (7)$$

If the terms $a_E^u u_E'$ and $a_W^u u_W'$ in Eq. (5) are neglected, the following equation for velocity correction is obtained:

$$u_P' = D_P (p_P' - p_E') \quad (8)$$

Received Aug. 15, 1992; revision received June 14, 1993; accepted for publication July 26, 1993. Copyright © 1993 by the American Institute of Aeronautics and Astronautics, Inc. All rights reserved.

*Head, Department of Mechanical Engineering, Private Bag X6001.

†Professor, Department of Mechanical Engineering, Private Bag X6001. Member AIAA.